

# Mathematical modeling and simulation of nanopore blocking by precipitation

M.-T. Wolfram<sup>1</sup>, M. Burger<sup>2</sup> and Z. S. Siwy<sup>3</sup>

<sup>1</sup> Department of Applied Mathematics and Theoretical Physics, Wilberforce Road, CB3 0WA, Cambridge, UK

<sup>2</sup> Institut für Numerische und Angewandte Mathematik, Einsteinstr.62, 48149 Münster, Germany

<sup>3</sup> Department of Physics and Astronomy, University of California, Irvine, 210G Rowland Hall, Irvine, CA 92697, USA

E-mail: M.Wolfram@damp.cam.ac.uk, martin.burger@wwu.de, zsiwy@uci.edu

**Abstract.** High surface charges of polymer pore walls and applied electric fields can lead to the formation and subsequent dissolution of precipitates in nanopores. These precipitates block the pore, leading to current fluctuations.

We present an extended Poisson-Nernst-Planck system which includes chemical reactions of precipitation and dissolution. We discuss the mathematical modeling and present 2D numerical simulations.

AMS classification scheme numbers:

Submitted to: *JPCM*

## 1. Introduction

Nanopores attracted a great deal of interests of scientists from various fields [1]. It is because nanopores are characterized by transport properties, which cannot be observed in microscale systems. Ionic and molecular selectivity [2, 3, 4, 5, 6], ion current rectification [7, 8, 9, 10, 11, 12, 13], and a diode behavior [14, 15, 16] are only a few of nanoeffects recorded with nanopores. Ionic concentrations in nanopores are often different from corresponding values in the bulk solution [17]. Surface charge of the pore walls and applied electric field can lead to increase of ionic concentrations inside a pore. If a nanopore is in contact with a solution of weakly soluble salt, ionic concentrations inside the pore can increase above the level dictated by the solubility product of this compound so that precipitates form and effectively plug the pore. This phenomenon has recently been observed in conically shaped polymer nanopores as a voltage-induced drop of the transmembrane current [18, 19]. The precipitates were found very unstable and their subsequent formation followed by dissolution resulted in ion current fluctuations in time. The characteristic feature of these voltage-induced ion current instabilities is

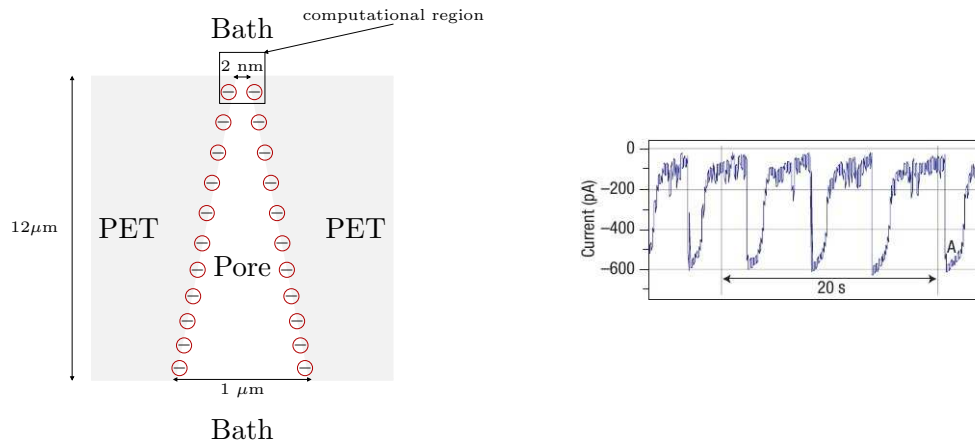


Figure 1: Left: Sketch nanopore (not in scale), right: current oscillations [19]

the existence of a voltage threshold, which defines the onset of the unstable regime. The current fluctuations have also a different shape compared to ion current switching observed in biological channels of a cell membrane [20]. The biological channels produce rectangular shaped opening and closing of the channel, indicating a very rapid kinetics of the processes responsible for the current changes. The precipitation-induced current instabilities resemble in their shape electrochemical fluctuations observed in other electrochemical systems [21]. Namely, the current spikes have a very asymmetric shape: there is a quick increase of the current followed by much slower process of pore closing, which we attribute to the nanoprecipitates formation. The current instabilities produced by conical nanopores are also very periodic, especially at higher applied voltages. The oscillating conical nanopores produce the fastest electrochemical oscillations observed so far, offering frequencies between fractions of Hz up to tens of Hz. Different approaches can be found in literature to describe particular features of nanopores with the desired complexity, i.e. the stationary PNP equations to calculate the current through nanopores [17, 22], a coupled Monte-Carlo PNP model to describe the anomalous mole fraction effect [23], or Molecular Dynamics simulation to model the ion current rectification in silica nanopores [24]. Few results can be found in the mathematical literature on mathematical models for precipitation and dissolution, e.g. crystal dissolution and precipitation in porous media [26, 27]. In this publication we present the first application of the PNP equations coupled with chemical reactions applied to ion current instabilities observed in nanoporous systems. The model gives insight into the kinetics and microscopic picture of the nanopore with transient precipitates. We believe that the developed approach can be applied to other nanoporous systems in which current instabilities have been observed.

## 2. Mathematical modeling of nanopores - the extended Poisson-Nernst-Planck equations

Our proposed mathematical model is based on the 2D PNP equations, which assume that the main driving forces for the ions are the diffusion and the electrostatic interaction with other ions and the surface charges on the pore walls. The PNP equations are a standard model for electrodiffusion of ions, cf. [28], their application to ion channels has been discussed e.g. in [29, 30, 31], and to nanopores e.g. in [22, 17]. The general formulation of the PNP equations is given by:

$$\operatorname{div}(\varepsilon \nabla V) = e \sum_{k=0}^m z_k \rho_k \quad (1a)$$

$$\frac{\partial \rho_k}{\partial t} = \operatorname{div} J_k \quad \forall k = 1, \dots, m \quad (1b)$$

$$J_k = -\frac{1}{k_B T} D_k(x) \rho_k \nabla \mu_k \quad \forall k = 1, \dots, m \quad (1c)$$

$$\mu_k = \mu_k^0 + z_k e V + k_B T \log(\rho_k) + \mu_k^{ex} \quad \forall k = 1, \dots, m, \quad (1d)$$

where  $\rho_k$  is the concentration of the  $k$ -th ionic species and  $V$  the electric potential. The total number of different species present in the system is denoted by  $m$ . We refer to  $D_k$  as the diffusion coefficient of every species,  $z_k$  is the corresponding valence. The parameter  $k_B$  is the Boltzmann constant,  $T$  denotes the temperature,  $\varepsilon$  the dielectric coefficient and  $e$  the elementary charge. We refer to  $\mu_k$  (1d) as the electrochemical potential, which includes electrostatic interaction (second term), diffusion (third term), external forces via a potential  $\mu_k^0$  and finite size effects via  $\mu_k^{ex}$  (excess chemical potential). The potential  $\mu_k^{ex}$  can be calculated e.g. using density functional theory (DFT) for fluids [29] or mean spherical approximations, see [31].

The general PNP equations (1a)-(1d) serve as a basis for our extended mathematical model including precipitation and dissolution. Precipitation denotes the mean formation of an insoluble solid in a liquid as a result of chemical reaction between two or more soluble substances. As an example we discuss the formation of cobalt hydrogen phosphate  $\text{CoHPO}_4$ . Precipitation can only occur if

$$K_{sp} < a_{\text{Co}^{2+}} a_{\text{HPO}_4^{2-}}, \quad (2)$$

where  $a_{\text{Co}^{2+}}$  and  $a_{\text{HPO}_4^{2-}}$  denotes the activity of the ionic species in equilibrium and  $K_{sp}$  the solubility equilibrium constant. On the other hand if  $K_{sp} > a_{\text{Co}^{2+}} a_{\text{HPO}_4^{2-}}$  then  $\text{CoHPO}_4$  dissolves into its component parts  $\text{Co}^{2+}$  and  $\text{HPO}_4^{2-}$ . The activity of a species is directly proportional to its concentration, i.e.

$$a_{\text{Co}^{2+}} = \gamma_{\text{Co}^{2+}} \rho_{\text{Co}^{2+}} \quad \text{and} \quad a_{\text{HPO}_4^{2-}} = \gamma_{\text{HPO}_4^{2-}} \rho_{\text{HPO}_4^{2-}},$$

where  $\gamma_{\text{Co}^{2+}}$  and  $\gamma_{\text{HPO}_4^{2-}}$  denote the activity coefficients,  $\rho_{\text{Co}^{2+}}$  and  $\rho_{\text{HPO}_4^{2-}}$  the concentrations. Note that the activity of a species depends heavily on the temperature and that the activity of a pure solid equals one by definition. Different models for the calculation of the activity coefficients can be found in literature, we concentrate on the

Brønsted-Guggenheim-Scatchard specific interaction theory [32, 33, 34].

The rate of a chemical reaction can be quantified by the precipitation and dissolution rate  $k_p$  and  $k_d$  respectively. Then the formation of  $\text{CoHPO}_4$  can be written as the following system of ordinary differential equations (in absence of other effects)

$$\frac{\partial \rho_{\text{Co}^{2+}}}{\partial t} = -k_p \rho_{\text{Co}^{2+}} \rho_{\text{HPO}_4^{2-}} + k_d \rho_{\text{CoHPO}_4} \quad (3a)$$

$$\frac{\partial \rho_{\text{HPO}_4^{2-}}}{\partial t} = -k_p \rho_{\text{Co}^{2+}} \rho_{\text{HPO}_4^{2-}} + k_d \rho_{\text{CoHPO}_4} \quad (3b)$$

$$\frac{\partial \rho_{\text{CoHPO}_4}}{\partial t} = k_p \rho_{\text{Co}^{2+}} \rho_{\text{HPO}_4^{2-}} - k_d \rho_{\text{CoHPO}_4} \quad (3c)$$

with given initial concentrations for  $\rho_{\text{Co}^{2+}}$ ,  $\rho_{\text{HPO}_4^{2-}}$  and  $\rho_{\text{CoHPO}_4}$ .

These reaction equations can be included into the PNP system. Let  $\rho_1$  and  $\rho_2$  denote the concentration of the soluble ions participating in the chemical reaction (e.g.  $\text{Co}^{2+}$  and  $\text{HPO}_4^{2-}$  ions),  $\rho_3$  the concentration of the solid species (e.g. cobalt hydrogen phosphate  $\text{CoHPO}_4$ ) and  $\rho_4 \dots \rho_m$  other ions present in the solution. Then the extended PNP system reads

$$-\text{div}(\varepsilon \nabla V) = e \left( z_1 \rho_1 + z_2 \rho_2 + \sum_{k=4}^m z_k \rho_k \right) \quad (4a)$$

$$\begin{aligned} \frac{\partial \rho_1}{\partial t} = & \text{div} [D_1(\rho_3) (k_B T \nabla \rho_1 + z_1 \rho_1 \nabla V)] - \\ & - a(x) k_p \rho_1 \rho_2 + (1 - a(x)) k_d \rho_3 \end{aligned} \quad (4b)$$

$$\begin{aligned} \frac{\partial \rho_2}{\partial t} = & \text{div} [D_2(\rho_3) (k_B T \nabla \rho_2 + z_2 \rho_2 \nabla V)] - \\ & - a(x) k_p \rho_1 \rho_2 + (1 - a(x)) k_d \rho_3 \end{aligned} \quad (4c)$$

$$\frac{\partial \rho_3}{\partial t} = \text{div} [D_3(\rho_3) (k_B T \nabla \rho_3)] + a(x) k_p \rho_1 \rho_2 - (1 - a(x)) k_d \rho_3 \quad (4d)$$

$$\frac{\partial \rho_k}{\partial t} = \text{div} [D_k(\rho_3) (k_B T \nabla \rho_k + z_k \rho_k \nabla V)] \quad k = 4, \dots, m. \quad (4e)$$

Note that except the reduced mobility due to formation of precipitates we do not include any finite size effects or external potentials at this point, i.e.  $\mu_k^{ex} = \mu_k^0 = 0$  in (1d). The diffusion coefficients  $D_i$ ,  $i = 1, \dots, m$  depend on the density of the solid  $\rho_3$ , modeling the blocking of the pore. We model them of the form

$$D_k(\rho_3(x), x) = \tilde{D}_k(x) m(\rho_3(x)) \quad \text{with} \quad m(\rho) = 2 \frac{e^{-\gamma \rho}}{1 + e^{-\gamma \rho}}, \quad (5)$$

where  $\tilde{D}_k(x)$  denotes the diffusivity in the pore and bath. Note that the function  $m(\rho(\cdot))$  decreases exponentially with  $\phi_3$ , i.e. the higher the concentration of the precipitate the lower the diffusivity. The dependence of diffusion coefficients on the precipitate concentration can be thought of as a limit of a diffusion coefficient depending on the total volume occupied by all species such as in the modified PNP model with size effects discussed in [35]. The coefficient  $a(x)$  is determined by the activity of the solution

$$a(x) = \begin{cases} 1 & a_1(x) a_2(x) > K_{sp} \\ 0 & a_1(x) a_2(x) < K_{sp} \end{cases}$$

where  $a_1(x)$  and  $a_2(x)$  are the activities of  $\rho_1$  and  $\rho_2$  respectively and  $K_{sp}$  is the solubility constant. The carboxyl charges on the inside of the pore wall are modeled using Neumann boundary conditions, namely

$$\varepsilon \frac{\partial V}{\partial n} = \sigma \quad \forall x \in \Gamma_p. \quad (6)$$

For the different species we fix the applied voltage  $U$  and the ionic concentrations in the bath

$$\begin{aligned} \rho_k &= \eta_k \quad \forall x \in \Gamma_D, \\ V &= U \quad \forall x \in \Gamma_D. \end{aligned}$$

On the remaining part of the boundary we model insulation using homogeneous Neumann boundary conditions. Based on Equation (6), we choose the following scaling

$$x = Lx_s \quad V = \tilde{V}V_s \quad \sigma = \tilde{\sigma}\sigma_s,$$

where  $L$  denotes the typical length,  $\tilde{V}$  the typical voltage and  $\tilde{\sigma}$  the typical density of surface charge density. Then the scaled Neumann boundary condition Equation (6) is given by

$$\left( \frac{\varepsilon \tilde{V}}{\tilde{\sigma} L} \right) \frac{\partial V_s}{\partial n_s} = \sigma_s.$$

Therefore we choose the effective parameter  $\lambda$  to be

$$\lambda^2 = \frac{\varepsilon \tilde{V}}{L \tilde{\sigma}}.$$

Then the scaled system (4a)-(4e) reads as (omitting the subscript s)

$$-\lambda^2 \Delta V = \kappa [(z_1 \rho_1 + z_2 \rho_2) + \sum_{k=4}^m z_k \rho_k] \quad (7a)$$

$$\begin{aligned} \frac{\partial \rho_1}{\partial t} &= \text{div} [D_1(\rho_3) (\nabla \rho_1 + cz_1 \rho_1 \nabla V)] - \\ &\quad - a(x) k_p \rho_1 \rho_2 + (1 - a(x)) k_d \rho_3 \end{aligned} \quad (7b)$$

$$\begin{aligned} \frac{\partial \rho_2}{\partial t} &= \text{div} [D_2(\rho_3) (\nabla \rho_2 + cz_2 \rho_2 \nabla V)] - \\ &\quad - a(x) k_p \rho_1 \rho_2 + (1 - a(x)) k_d \rho_3 \end{aligned} \quad (7c)$$

$$\frac{\partial \rho_3}{\partial t} = \text{div} [D_3(\rho_3) (\nabla \rho_3)] + a k_p \rho_1 \rho_2 - (1 - a) k_d \rho_3 \quad (7d)$$

$$\frac{\partial \rho_k}{\partial t} = \text{div} [D_k(\rho_3) (\nabla \rho_k + cz_k \rho_k \nabla V)] \quad (7e)$$

where  $\kappa = \frac{eL\tilde{\rho}}{\tilde{\sigma}}$ ,  $c = \frac{eV}{k_B T}$  and  $\tilde{\rho}$  denotes the typical concentration of the ionic species.

### 3. Numerical scheme

We use the following Gummel-type procedure to solve the PNP equations (7a)-(7e) at every time step  $t = t_j$ . Here  $V_j$  and  $\rho_{k,j}$  denote the potential and the k-th ionic species at time  $t = t_j$  respectively.

j	1	2	3	4	5
Species	Co	$\text{HPO}_4^{2-}$	$\text{CoHPO}_4$	Cl	K
Charge	2e	-2e	0	-e	e
Left bath $\rho_j$	1 mM	1 mM	0 mM	2 mM	1 mM
Right bath $\rho_j$	1 mM	1 mM	0 mM	2 mM	1 mM

Table 1: Values for the Dirichlet boundary conditions

- Solve the Poisson equation (7a) for the potential  $V_j$
- Solve the Nernst-Planck equations (7b)-(7e) for  $\rho_{k,j}$  in an iterative manner using the potential  $V_j$ .

The Poisson equation (7a) can be solved using a standard hybrid discontinuous Galerkin (DG) method. The Nernst-Planck equations (7b)-(7e) are solved using a semi-implicit discretization in time. For the sake of readability we only state the semi-discrete equation for  $\rho_1$  given by

$$\frac{\rho_{1,j} - \rho_{1,j-1}}{\Delta t} + \text{div} [D_1 (\rho_{3,j-1}) (\nabla \rho_{1,j} + cz_1 \rho_{1,j} \nabla V)] = (-a(x)k_p(x)\rho_{1,j-1}\rho_{2,j-1} + (1 - a(x))k_d\rho_{3,j-1}(x)). \quad (8)$$

Here  $\Delta t$  denotes the time steps  $\Delta t = t_j - t_{j-1}$ . Equations (7b)-(7e) are solved using a mixed stabilized DG method introduced in [36]. For a detailed presentation of the numerical scheme we refer to [37].

#### 4. Simulations

Nanopores have different length scales - the length of the pore is in the micrometer range, the narrow opening in the nanometer range, resulting in a multiscale problem. Since the plugging of the pore happens at its narrow tip, we consider only the narrow opening part in our calculations (see Figure 1).

We choose a tapered cone of length  $L = 50$  nm with opening radii  $d_1 = 2$  nm and  $d_2 = 3$  nm. The radii correspond to the opening angle  $\theta \approx 1^\circ$  of actual nanopores. The computational geometry consists of the small cone tip as well as two attached conical shaped bath regions. The typical length is set to  $L = 1$  nm, the typical concentration  $\tilde{\rho} = 1$  mM and the typical surface charge to  $\tilde{\sigma} = 1 \frac{\text{e}}{\text{nm}^2}$ .

The generalized PNP system (7a)-(7e) involves five species, the dissolved ions  $\text{Co}^{2+}$ ,  $\text{K}^+$ ,  $\text{Cl}^-$  and  $\text{HPO}_4^{2-}$  as well as the precipitate  $\text{CoHPO}_4$ . The bulk solubility product  $K_{sp} = 2 \times 10^{-7} \frac{\text{mol}}{\text{dm}^3}$  is taken from [38], the scaled precipitation and dissolution rates are chosen to be  $k_p = k_d = 2$ .

The boundary conditions for the concentrations are chosen such that the charge neutrality condition  $\sum_{k=0}^m z_k \rho_k = 0$  is satisfied (see Table 1). The initial conditions are

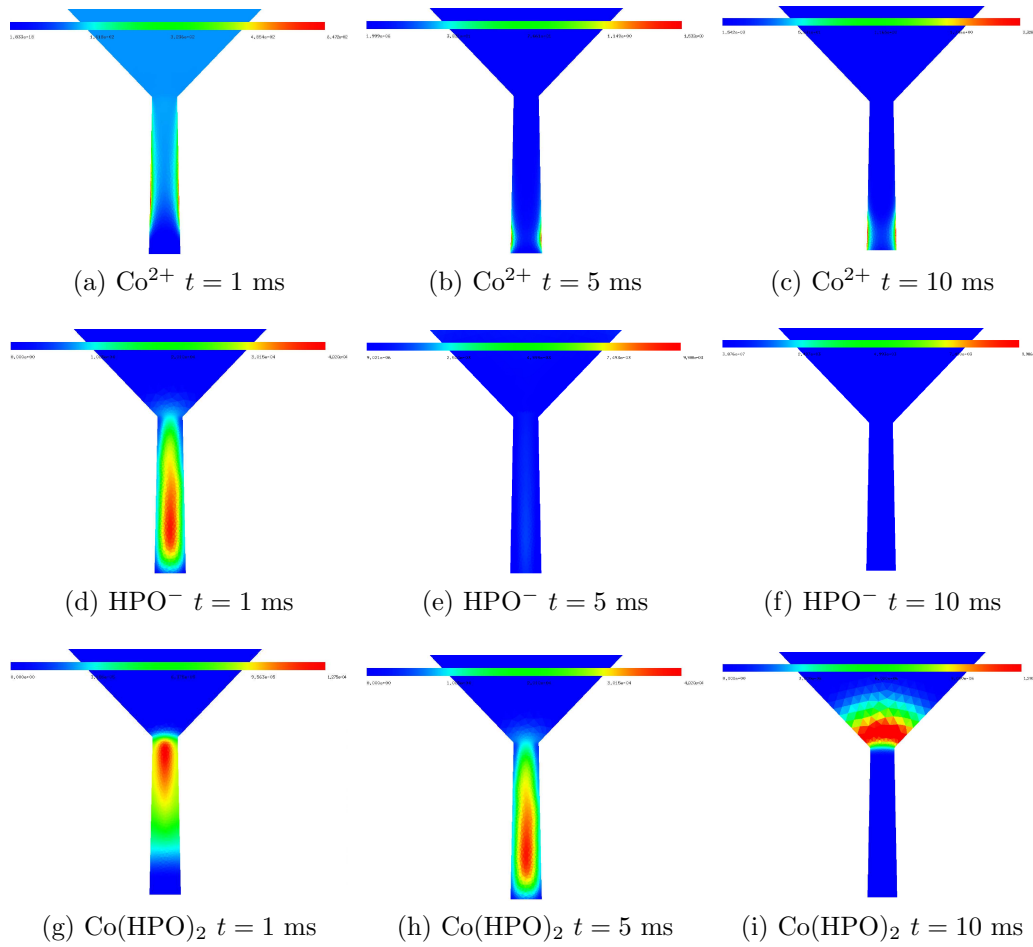


Figure 2: Formation of a plug as a function of time

set to

$$\rho_k(x, 0) = \begin{cases} \eta_{k,r} & \text{for all } x \text{ in the right bath} \\ \eta_{k,l} & \text{for all } x \text{ in the left bath} \\ 0 & \text{inside the pore} \end{cases} \quad (9)$$

where  $\eta_{k,r}$  and  $\eta_{k,l}$  denote the Dirichlet boundary values respectively.

Figure 2 illustrates the formation of a plug in the nanopore (only the very narrow tip and the parts of the attached bath are shown in the picture). The plug originates in the center of the narrow tip and accumulates below the narrow tip. It causes a decrease in the diffusivity Equation (5) as well as in the measured current (see Figure 3). Note that the scaled density in Figure (2i) is much smaller than in (2g) and (2h). Furthermore we observe that the plugging of the pore happens on the same time scale as the experiments, it takes about 5 ms until the plug starts to dissolve.

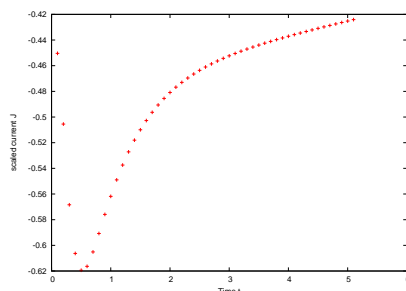


Figure 3: Decrease of ion current in time

## 5. Conclusions and further work

We presented an extended PNP model which provides the first insight into the kinetics of formation and dissolution of precipitates inside a single conically shaped nanopore. First numerical simulations show good agreement with experimental data, i.e. the plug formation happens on same time scale as well as no formation and subsequent dissolution for less soluble compounds like  $\text{Mg}(\text{OH})_2$ . Our studies also raise a number of interesting questions e.g.

- What are other possible models for the formation and dissolution of a plug ?
- What are appropriate values for the precipitation and dissolution rate of the precipitates in a nanopore?
- Do the solubility products in nanopores differ from their values in the bulk?

These questions pose further challenges for mathematicians and experimentalists. Different mathematical approaches could apply various thresholds in order to describe the formation of the plug. Another interesting feature is the asymmetric shape of the current fluctuations: the pore opening occurs on a much faster time scale than the plugging. This observation might point to yet another mechanism for the pore opening. It is possible that the precipitate formation increases the pressure inside the pore, which leads to the precipitate being "ejected". In order to study this option, the presented model would have to be complemented by additional equations, e.g. by coupling PNP with the Navier-Stokes equations or at least by assuming that the diffusion coefficient  $D_k$  depends on the pressure.

## References

- [1] Dekker C 2001 *Nat. Nanotech.* **2** 209-215
- [2] Plecis A, Schoch R B, and Renaud P 2005 *Nano Lett.* **5** 1147-55
- [3] Nishizawa , Martin C R, and Menon V P 1995 *Science* **268** 700-702
- [4] Vlassiuk I, Smirnov S, and Siwy Z S 2008 *Nano Lett.* **8** 1978-85
- [5] Kohli P, Harrell C, Cao C Z, Gasparac R, Tan W, and Martin C R 2004 *Science* **305** 984-986
- [6] Howorka S, and Siwy Z S 2009 *Chem. Soc. Rev.* **38** 2360-84
- [7] Wei C, Bard J and Feldberg S W 1997 *Anal. Chem.* **69** 4627-46

- [8] Apel P Y, Korchev Y E, Siwy Z, Spohr R and Yoshida M 2001 *Nucl. Instrum. Methods Phys. Res. B* **184** 337-346
- [9] Siwy Z S, and Fulinski A 2002 *Phys. Rev Lett.* **89** 1981031-4
- [10] While H S, and Bund A 2008 *Langmuir* **24** 12062-67
- [11] Umehara S, Pourmand N, Webb C D, Davis R W, Yasuda K, and Karhanek M 2006 *Nano Lett.* **6** 2486-92
- [12] Siwy Z S, Heins E, Harrell C C, Kohli P, and Martin C R 2004 *J. Am. Chem. Soc.* **126** 10850-51
- [13] Siwy Z S, and Howorka S 2010 *Chem. Soc. Rev* DOI 10.1039/b909105j
- [14] Vlassioux I, and Siwy Z S 2007 *Nano Lett.* **7** 552-56
- [15] Karnik R, Duan C H, Castelino K, Daiguji H, and Majumdar A 2007 *Nano Lett.* **7** 547-51
- [16] Cheng L J, and Guo L J 2009 *ACS Nano* **3** 575-84
- [17] Cervera J, Schiedt B, and Ramírez P 2005 *EPL (Europhysics Letters)* **71** 35-41
- [18] Siwy Z, Powell M R, Petrov A, Kalman E, Trautmann C, and Eisenberg R S (2006) *Nano Lett.* **6** 1729-34
- [19] Powell M R, Sullivan M, Vlassioux I, Constantin D, Sudre O, Martens C C, Eisenberg R S and Siwy Z S 2008 *Nature Nanotech.* **3** 51-57
- [20] Hille B 2001 *Ion channels of excitable membranes* Sinauer Associates
- [21] Degn H 1968 *Transaction of the Faraday Society* **64** 1348-1358
- [22] Cervera J, Schiedt B, Neumann R, Mafe S, and Ramirez P 2006 *J. Chem. Phys.* **124** 104706
- [23] Gillespie D, Boda D, He Y, Apel P and Siwy Z S 2008 *Biophys. J.* **95** 609-19
- [24] Cruz-Chu E R, Aksimentiev A and Schulten K 2009 *Journal of Phys. Chem. C* **113** 1850-62
- [25] Cruz-Chu E R, Ritz T, Ziwy Z S and Schulten K 2009 *Faraday Discussion* **43** 1-16
- [26] Devigne V M, Pop I S, van Duijn C J and Clopeau T 2008 *SIAM J. Numer. Anal.*, **46** 895-919
- [27] Maise E and Pousin J 1997 *J. Comput. Appl. Math.*, **82** 279-90
- [28] Rubinstein I 1990 *Electro-Diffusion of Ions* (Society for Industrial and Applied mathematics)
- [29] Gillespie D, Nonner W, and Eisenberg R S 2002 *J. Phys.: Condens. Matter* **14** 12129-45
- [30] Gillespie D, Nonner W, and Eisenberg R S 2003 *Phys. Rev. E* **68** 031503
- [31] Nonner W, Catacuzzeno L and Eisenberg R S 2000 *Biophys. J.* **79** 1976-92
- [32] Guggenheim E A 1934, *Phil. Mag* **19** 588-643
- [33] Scatchard G 1976, *Equilibrium in Solutions: Surface and Colloid Chemistry* (Harvard University Press)
- [34] Ciavatta L 1980, *Annali di Chimica* **70** 551-67
- [35] Burger M, Schlake B 2010, Nonlinear Poisson-Nernst-Planck equations for flux through confined geometries, Preprint.
- [36] Egger H and Schöberl J 2009 *IMA. J. Num. Anal.*
- [37] Wolfram M.-T. 2008 *Forward and Inverse Solvers for Electrodiffusion Systems* (PhD Thesis, University of Linz)
- [38] Dean J A 1998 *Lange's Handbook of Chemistry* (McGraw-Hill Professional)

## Acknowledgments

MB has been supported by the Volkswagen Stiftung, Grant Nr. I/83-928. MTW has been supported by Award No. KUK-I1-007-43, made by King Abdullah University of Science and Technology (KAUST). The authors thank R.S.Eisenberg (Rush Medical University) for useful and stimulating discussions.